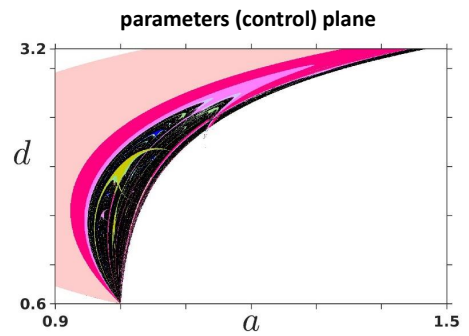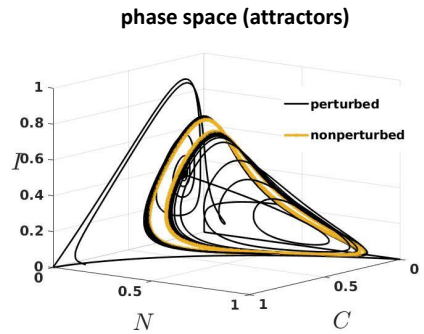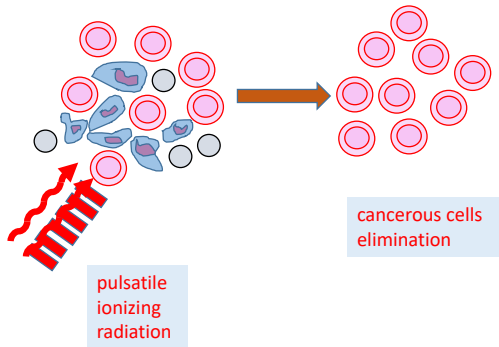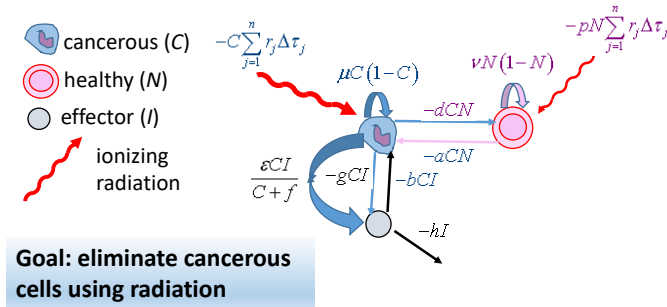# Graphical Abstract

Exploring chronomodulated radiotherapy strategies in a chaotic population model

Gonzalo Marcelo Ramírez-Ávila,Juergen Kurths,Didier Gonze,Geneviève Dupont

Highlights

Exploring chronomodulated radiotherapy strategies in a chaotic population model

Gonzalo Marcelo Ramírez-Ávila,Juergen Kurths,Didier Gonze,Geneviève Dupont

- Analysis of a nonlinear dynamical system describing cancerous-healthy cell competition

- Examination of how ionizing radiation acts on the cell competition dynamics

- Key role of the irradiation protocol and its precise dosing time in the cell dynamics

- Possible irradiation time reduction and the total dose delivered in radiotherapy

- Numerical results support the chronobiology role in radiotherapy and its effectiveness

Exploring chronomodulated radiotherapy strategies in a chaotic population model

Gonzalo Marcelo Ramírez-Ávila[a,b,*], Juergen Kurths[c,d], Didier Gonze[b] and Geneviève Dupont[b]

[a]*Instituto de Investigaciones Físicas, Universidad Mayor de San Andrés, La Paz, Bolivia*

[b]*Unit of Theoretical Chronobiology, Université Libre de Bruxelles, CP231, Boulevard du Triomphe, 1050 Brussels, Belgium*

[c]*Potsdam Institute for Climate Impact Research (PIK), 14473 Potsdam, Germany*

[d]*Institut für Physik, Humboldt-Universität zu Berlin, 10115 Berlin, Germany*

ABSTRACT

We present a simple nonlinear model describing the population dynamics of cancerous, healthy, and effector cells submitted to ionizing radiation. We examine the situations in which intermittently high doses of radiation affect the cells as it occurs in radiotherapy. The model explores various irradiation parameters, such as the total delivered dose for a given standard dose rate and the number of treatment sessions seeking situations that optimize normal cells survival. In other words, we are interested in enhancing the effectiveness of a radiotherapy treatment by adjusting the temporal pattern of the dose deliverance through an exhaustive dynamical characterization of the system. This includes the study of the parameter planes, the populations' dynamical behavior going from fixed points to chaotic oscillations, and the basins of attraction. This work leads to counter-intuitive predictions and constitutes a step towards a model of chronomodulated radiotherapy.
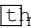
1. Introduction

Cancer is one of the most common and lethal pathologies in humans and constitutes a significant health problem. According to the World Health Organization (WHO), in 2020, the last year of available data, around 1.93×10^7 new cases were registered, having an estimated mortality of almost 1×10^7, constituting approximately 1/6 of total human deaths in the world [1]. Among the treatments used to fight cancer, there are those based on purely medical (surgery [2]), physical (radiotherapy [3, 4, 5, 6, 7]), chemical (chemotherapy [8, 9, 10, 11]), biological (immunotherapy [12, 13], targeted gene therapy [14], oncolytic [15] and hormonal) aspects, and combinations of the above mentioned. Cancer has acquired singular importance in recent decades due to its impact on society and the efforts dedicated to combating it. One way to understand the processes underlying the development of tumors is through experiments and models that can explain the experimental results and make predictions of various situations that are not easily accessible to measurements. Thus, different scientific groups have begun to formulate models of tumor growth or proliferation of cancerous cells [16, 17, 18, 19, 20]. In addition, the population dynamics of cancer cells consider their interaction with other cell types or/and different external agents acting on tumors. Most models display typical nonlinear behaviors such as chaos and multistability [21, 22]. The occurrence of multistability in several contexts has

been extensively reviewed in [23], including those concerned with cancer attractors [24, 25].

Several models have been proposed to study different situations linked to tumors (macroscopic approach) and cancer cells (microscopic vision). A paradigmatic model used in cancer cells' population dynamics considers immunogenic tumors and the calculation of local and global bifurcations as a function of relevant biological parameters [26]. Along the same lines, another famous model proposed by Kirschner & Panetta [27] consists of a system of three ordinary differential equations (ODEs) related to the population of immune cells, tumor cells, and the concentration of interleukin-2 cytokine (IL-2), a compound that activates the immune system to fight tumors. Finally, it is noteworthy to mention similar models based on adaptive cellular immunotherapy (ACI) with similar characteristics. In particular, Nani & Freedman [28] have proposed an extension of the previous models, having as main variables the normal and cancerous cell concentrations in the physiological space, as well as the concentrations of lymphokine (e.g., IL-2) and anticancer lymphocytes (such as lymphokine-activated killer cells) in the vicinity of normal and cancerous cells.

The importance of radiotherapy in the treatment, control, and as a palliative of cancer disease is essential [6], and there are efforts to expand global access to this type of treatment. Approximately 50% of patients must follow radiotherapy to treat cancer. Concerning the models involving radiotherapy, they often describe the competition between healthy and cancerous cells by the Lotka-Volterra equations. The exposure of the cancerous cells to radiation is done following four modes: constant, linear, feedback, and periodic. It is also possible to take into account the action of radiation on healthy cells [29] and to describe the spatio-temporal evolution of cells as 2-D [30, 31] or 3-D nonlinear dynamical systems [32]. Another approach is given by multiscale models for cancer to improve radiotherapies [33]. In addition, some other tumor growth models have been considered, such as the Gompertz and the so-called "universal" exponential one [18]. There are also models combining two kinds of treatments, for instance, the simultaneous consideration of chemotherapy and radiotherapy in which the exhaustive analysis of the model equations confirms that treatments might actively modify the cancer dynamics [34]; and the combination of immunotherapy and radiotherapy [35].

Nowadays, chronobiology is a thriving research field with the remarkable quality of spanning almost every biomedical discipline from molecular biology and metabolism to psychology and internal medicine [36] and also including the use of mathematical models to elucidate the molecular bases of the involved rhythms and of their interplay with the other processes they interfere with [37]. This theoretical approach, closely based on experimental data, contributes to a thorough and deep understanding of the oscillatory phenomenon. Moreover, theoretical models lead to predictions that can, in turn, be tested experimentally. For chemotherapy, it has been demonstrated that adjusting the drug-delivery time in treatment increases both their efficacy and tolerability [38]. The prediction of the optimal temporal pattern of administration of anticancer drugs has often been accompanied by mathematical modeling, that has acquired importance in recent years [39, 40, 41, 42, 43]. These studies pertain to a temporal adjustment of the

treatment depending on the circadian clock of the patients. In the present study, we analyzed by intensive computation a nonlinear dynamical system that describes the competition between healthy and cancerous cells in addition to extending the concept of temporal modulation of cancer treatment to the pulsatile pattern of radiotherapy, independently of the circadian rhythm.

With the above explanations related to the main concepts used in this work, we introduce the model and its details in Sect 2. Next, the methods and results are outlined in Sect. 3, where we also discuss the main findings of the work. Finally, in Sect. 4 we present main comments and conclusions and provide perspectives for further developments.

2. Model

As stated in Sect. 1, several models describe the cell population dynamics related to cancer. Regardless of the type of treatment, the cancer models used to consider Gompertzian [16] or logistic growth, being the most common [29, 31, 32, 34, 38, 44, 45, 46, 47, 48, 49, 50, 51, 52, 53, 54, 55, 56, 57, 58]. Among the models on radiotherapy, we focus on those based on the action of the radiation on the cells as for instance [18, 30, 31, 32, 34, 56, 58, 59, 60]. Concretely, we use a model similar to that introduced in [46] but with radiation terms both for the cancerous and normal cells. The model scheme is shown in Fig. 1.

On the other hand, the radiation term must have the pulsatile feature because a typical radiotherapy treatment consists of several sessions with a much shorter duration than the whole treatment duration. Thus, the model describing the population density rate change of cancerous (C), normal or host (N), and immune effector (I) cells is given by:

$$\frac{dC}{dt} = \mu C (1 - C) - aCN - bCI - C \sum_{j=1}^{n} r_j \Delta \tau_j \,, \tag{1}$$

$$\frac{dN}{dt} = \nu N (1 - N) - dCN - pN \sum_{j=1}^{n} r_j \Delta \tau_j \,, \tag{2}$$

$$\frac{dI}{dt} = \frac{\varepsilon CI}{C + f} - gCI - hI \,, \tag{3}$$

where the parameters μ, ν and ε are related to the growth rate of C, N and I respectively. This growth rate is logistic for C and N and follows a Monod kinetics involving a constant f triggered by the presence of C for I. The competition parameters involving a reduction of C by N and I are a and b, respectively. Cancerous cells kill the normal and effector cells at rates given by d and g, respectively. The mortality of I is characterized by h. The meaning and further explanations of the parameters were widely described in [46, 49, 52]. Finally, the terms related to the pulsed action of ionizing radiation constitute a generalization of those introduced in [18, 30, 60], being $\Delta \tau_j = \delta(t - \tau_j)$, where δ stands for the Dirac function, indicating τ_j the time in which sessions occur, i.e., when the pulsed radiation is applied, and n is the number of irradiation sessions. As stated above, the irradiation time is quite
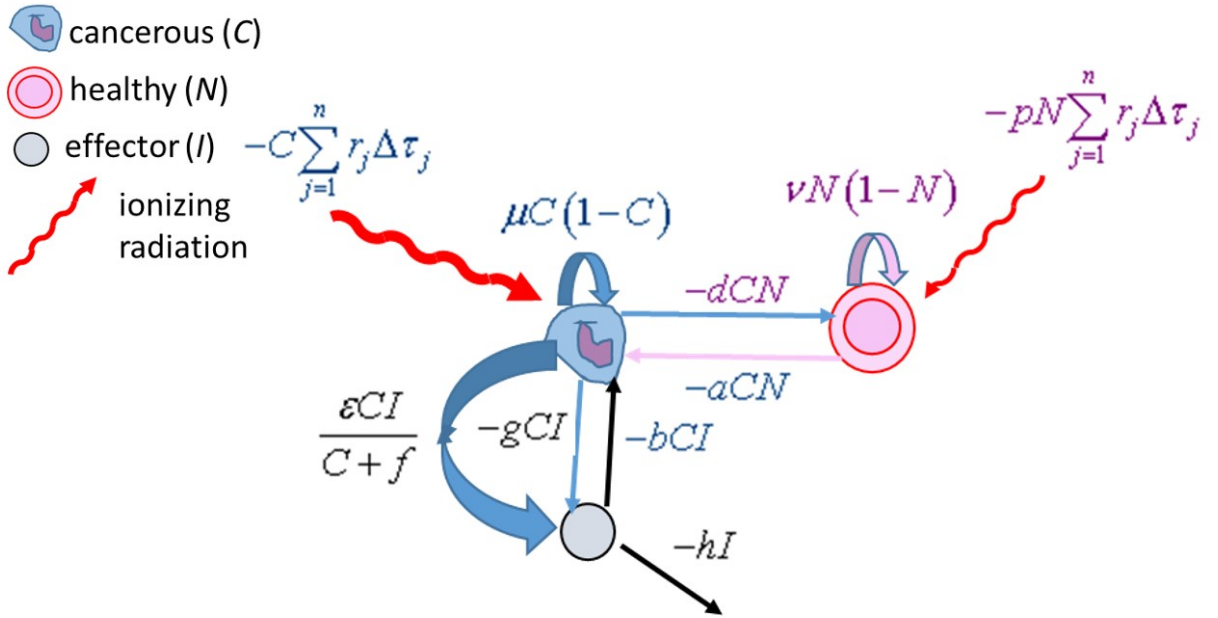
Figure 1: Model scheme. The direction of the arrows shows the action of one population on another. Next to the arrows, the consequent effect is described (the corresponding term in the set of equations), manifested by a population decrease in the affected cells, except when cancerous cells activate the presence of effector cells. Furthermore, ionizing radiation induces cell death, although it also affects the dynamics of cellular competition. Finally, the self-loops account for the population growth of each cell type.

short compared to the whole treatment duration, constituting the reason the irradiation term might be expressed using a Dirac δ function. The term r_j is related to (i) the total absorbed dose to be delivered during the whole treatment (D_T) in Gy (in radiation therapy, a typical value is of the order of 60 Gy [61]); (ii) the radiation beam absorbed dose rate in each session ($\dot{D}_j$), expressed in Gy/min (depending on the radiation sources, these values vary from 2-10 Gy/min [62, 63], we chose here 3 Gy/min); (iii) the duration of a session ($\Delta t_j = D_T/n\dot{D}_j$) in minutes; and (iv) the time interval between two consecutive sessions ($\Delta T_j = \tau_j - \tau_{j-1}$) in hours. Then, with the parameters mentioned above and a unitary dimensional factor κ in 1/[Gy-hr], which allows for estimating the effective action time in hours of the radiation on the cells. Thus, the radiation term r_j is determined by:

$$r_j = \kappa \dot{D}_j \frac{D_T}{n\dot{D}_j} = \kappa \dot{D}_j \Delta t_j .$$ (4)

Finally, the parameter p is related to the radiosensitivity of normal cells, depending on the irradiated organ. It is noteworthy to point out that this is a general form of the model that might be reduced to a more straightforward form under the assumption that $\Delta T_1 = \Delta T_2 = \cdots = \Delta T_n = \Delta T$, which indicates that the time interval between two

consecutive sessions is constant and also considering the constancy of both the radiation beam absorbed dose rate and the duration of each session: $\dot{D}_1 = \cdots = \dot{D}_n = \dot{D}$ and $\Delta t_1 = \cdots = \Delta t_n = \Delta t$, $r_j = r$ becomes constant too. Consequently, the irradiation term turns out:

$$\sum_{j=1}^{n} r_j \delta(t - \tau_j) = \sum_{j=0}^{n-1} r\delta(t - (j\tau + t_0)) \,, \tag{5}$$

with the occurrence of the first irradiation at time t_0.

The model, the parameter values, and the main features are adapted to the characteristic times in radiotherapy treatments.

3. Methods and results

Next, we analyze our model and explore the different possibilities driving us to improve the effectiveness of treatment. We start by choosing a and d as two relevant parameters for studying the system dynamics. This choice is made because the variation of the parameters mentioned above quantifies the competition between cancerous and healthy cells. The remaining parameters are set considering basic biological aspects, such as their positivity, and taking into account feasible values included in the stability intervals obtained in [59], in addition to a suitable choice of time scales in accordance with usual radiotherapy treatments. Therefore, considering the aspects above, the following parameter values are fixed: $\mu = 1$ hr^{-1}, $b = 2.5$ hr^{-1}, $v = 0.6$ hr^{-1}, $\varepsilon = 4.5$ hr^{-1}, $f = 1$, $g = 0.2$ hr^{-1}, $h = 0.5$ hr^{-1}. For simplicity, it is understood that the units of the parameters specified above are not changed; therefore, the units are not written from now on. Note that $\mu > v$ indicates that cancerous cells proliferate more than normal ones. On the other hand, the parameter related to the radiosensitivity p is a probability and, in principle, should be small ($p < 1$) due firstly to the fact that radioresistance is higher in normal cells and also because in an irradiation session, the protocol indicates that the adjacent regions of the tumor must be protected. Consequently, the absorbed dose of the areas constituted mainly by normal cells is much less. Therefore, we chose $p = 0.3$ for the reasons mentioned earlier. Concerning the other irradiation parameters related to the treatment protocol, we take, as indicated before, $D_T = 60$ Gy, $\dot{D} = 3$ Gy/min and $\kappa = 1/$(Gy-hr). Depending on the protocol, we adopt the values for n, t_0, τ, and ΔT permitting us to determine Δt and r. As a result, it is possible to integrate numerically Eqs. (1)–(3). In what follows, we show that despite the apparent simplicity of the model, it exhibits a huge variety of dynamic solutions depending on the parameters, initial conditions, and irradiation protocols. This points to the necessity of exploring the conditions allowing us to the most effective treatment, i.e., a treatment that simultaneously decreases the population of cancerous cells and maintains that of healthy cells.

3.1. Parameter planes and basins of attraction

Intending to get an in-depth insight into the system's dynamical behavior, we scanned the parameter planes by varying a and d to characterize the behavior for each combination of parameter values stated above. First, we used the initial conditions $(C(0), N(0), I(0))$ given by $(0.9, 0.09, 0.01)$ and $(0.09, 0.9, 0.01)$, for which we obtain the parameter planes of the healthy cells shown in Figs. 2(a)–(b). A comparison of Figs. $2(a)–b)evincesthattherearenosubstantialdifference$ $2 and 4 for cancerous cells, corresponding to period − 1 and 3 for healthy cells. The above mentioned situation is visualized in Fig. 2$ $−(f) because it indicates all the possible dynamical behavior of the system, including fixed point, periodic distinguishable until$ $20 and chaotic behaviors. In what follows, we will use this color code in the parameter planes and the basins of attraction. For the$ $order Runge − Kutta method with 4×10^6$ time steps of total integration, a transient of $2×10^6$ time steps, and a step time size of 0.01 hr^{-1}; the resolution of each panel is $1024×1024$ pixels. The detection of maxima and minima is made with a resolution of 10^{-6}. The bifurcation diagrams for a path among the infinity possible routes on the parameter plane display the dynamics for cancerous, normal, and effector cells as shown in Fig. 2(g)–(i) respectively. Note that the path, given by the straight line $d = 7.28 − 5.09a$ in the parameter plane, starts and finishes in the points $(a, d) = (0.97, 2.34)$ (period-1 dynamics) and $(a, d) = (1.08, 1.78)$ (fixed point) respectively (the diagonal in Figs. 2(d)–(e)), and traversing regions exhibiting different regular dynamics and also chaos. For cancerous and effector cells, the fixed point is close to zero and for normal cells, it is practically 1. We considered 8192 values of a and d, and each point corresponds to a peak or a valley of the time series. When there is a fixed point, the dynamical variable value remains constant.

The features stated above suggest the existence of multistability, i.e., the possibility of several dynamical behaviors according to the initial conditions [65]. To characterize such initial conditions dependence, we compute the basins of attraction of the regions observed above in Fig. 2 and some other regions, with emphasis on well-defined areas and zones where different dynamical behaviors are close to each other. First, we consider three cases corresponding to the right upper part of Fig. 2(a), namely when the parameter values (a, d) are respectively (1.383,3.177) (period-2), (1.383,3.109) (period-4), and (1.383,3.096) (chaos), but in Fig. 2(b) denote a fixed point. The basins of attraction for the values mentioned above of (a, d) are shown in Figs.3(a)–(c). The point $(a, d) = (1.103, 2.499)$ in the parameter plane corresponds to a point exhibiting a period-8 oscillatory behavior in Fig. 2(a). Thus, we expect again multistability that, in this case, displays some patterns in the basin of attraction depicted in Fig. 3(d) with the predominance of period-8 oscillatory behavior coexisting with chaos. In Fig. 3(e), where $(a, d) = (1.054, 2.308)$ (period-10) there are regions with periodicities multiples of five. Finally, when $(a, d) = (1.054, 2.285)$ (period-9), the basin of attraction is pervaded by period-9 as it is shown in Fig. 3(f). Notably, in the left part of the basins of attraction, there is a small strip with fixed point behavior, and in this region, the main issue is the predominance of healthy cells (almost 100%). The aspect mentioned above opens the possibility to lead the dynamical system towards the fixed point stability region by means of pulsatile perturbations related to the radiation, consequently eliminating the cancerous cells. The computa-
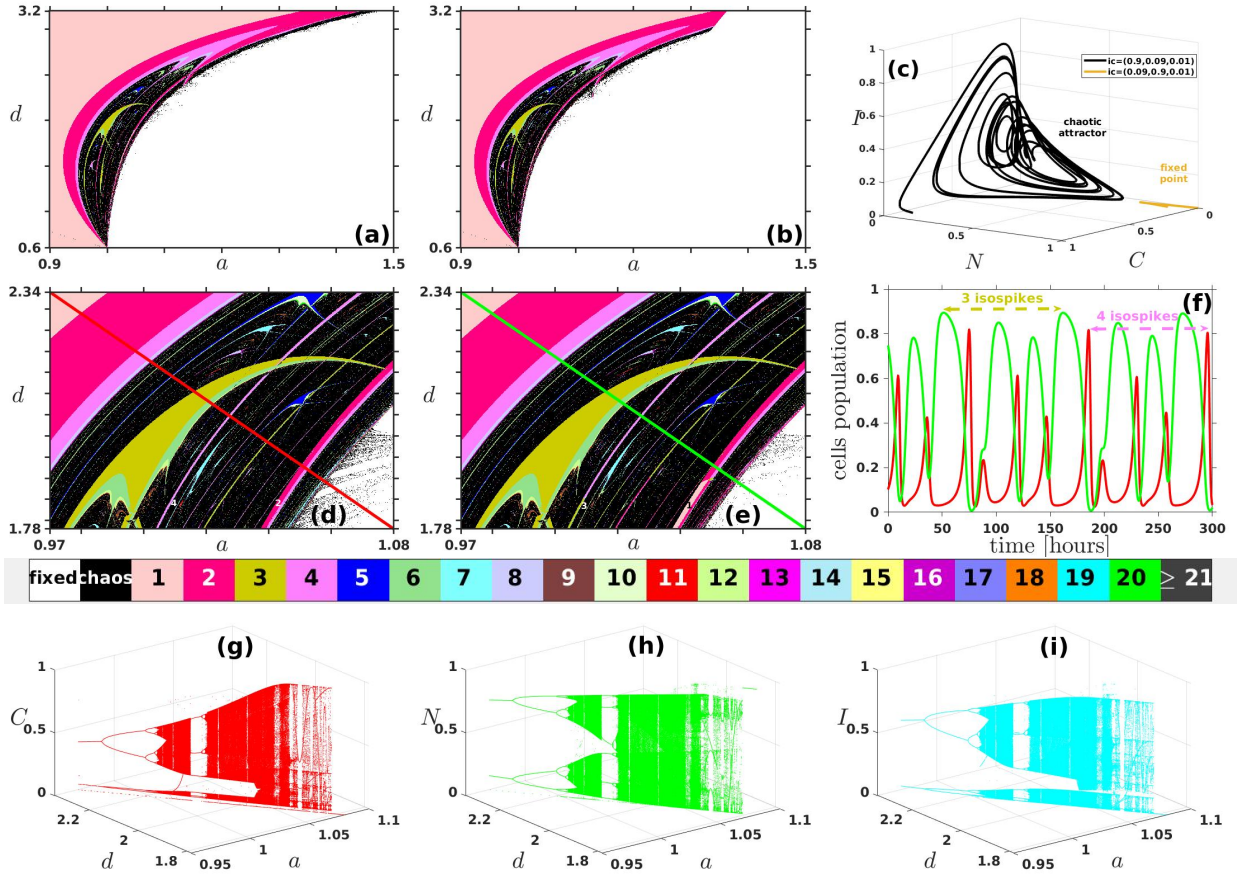
Figure 2: Parameter planes varying a and d for the dynamical system described by Eqs. (1)-(3) without the radiation terms and with the other parameter values given by $\mu = 1$, $b = 2.5$, $v = 0.6$, $\varepsilon = 4.5$, $f = 1$, $g = 0.2$, $h = 0.5$ (case of healthy cells N), when using the initial conditions (a) $(C(0), N(0), I(0)) = (0.90, 0.09, 0.01)$, and (b) $(C(0), N(0), I(0)) = (0.09, 0.90, 0.01)$. (c) Phase space obtained when $(a, d) = (1.362, 3.053)$, and the embedded manifolds when the initial conditions are those specified in (a) and (b) leading to a chaotic attractor and to a fixed point, respectively. Reduced regions of the parameter planes when the initial conditions are $(C(0), N(0), I(0)) = (0.5, 0.49, 0.01)$ for (d) cancerous, and (e) healthy cells. (f) Time series corresponding to cancerous (red) and healthy (green) cells when $(a, d) = (1.0084, 1.8375)$ with periods 4 and 3 as indicated in (d) and (e), respectively. Below, the color code is displayed for characterizing fixed point, chaotic, and different orders of periodicity featured by the number of isospikes in each period [64]. Bifurcation diagrams for a specific path given by the straight line $d = 7.28 - 5.09a$ (the diagonal going from $(a_1, d_1) = (0.97, 2.34)$ to $(a_2, d_2) = (1.08, 1.78)$) on the parameter planes (d)–(e), for (g) cancerous, (h) healthy, and (i) effector cells.

tional details for obtaining the basin of attractions are similar to those employed to obtain the parameter planes, except that for the basins of attraction, we considered 9.8×10^6 time steps of total integration, and a transient of 4.9×10^6 time steps. We considered the initial condition for the effector cells: $I(0) = 0.01$ in all cases.

### 3.2. Radiation effects on regular dynamical behavior

Here we analyze the situation where, according to the parameter plane results, a regular behavior is exhibited when no radiation is acting. First of all, we observe that there are wide regions where the system reaches a stable fixed point with predominant normal cells, as shown in Fig. 4(a) with $a = d = 1.1$. When we choose $a = d = 0.93$ with
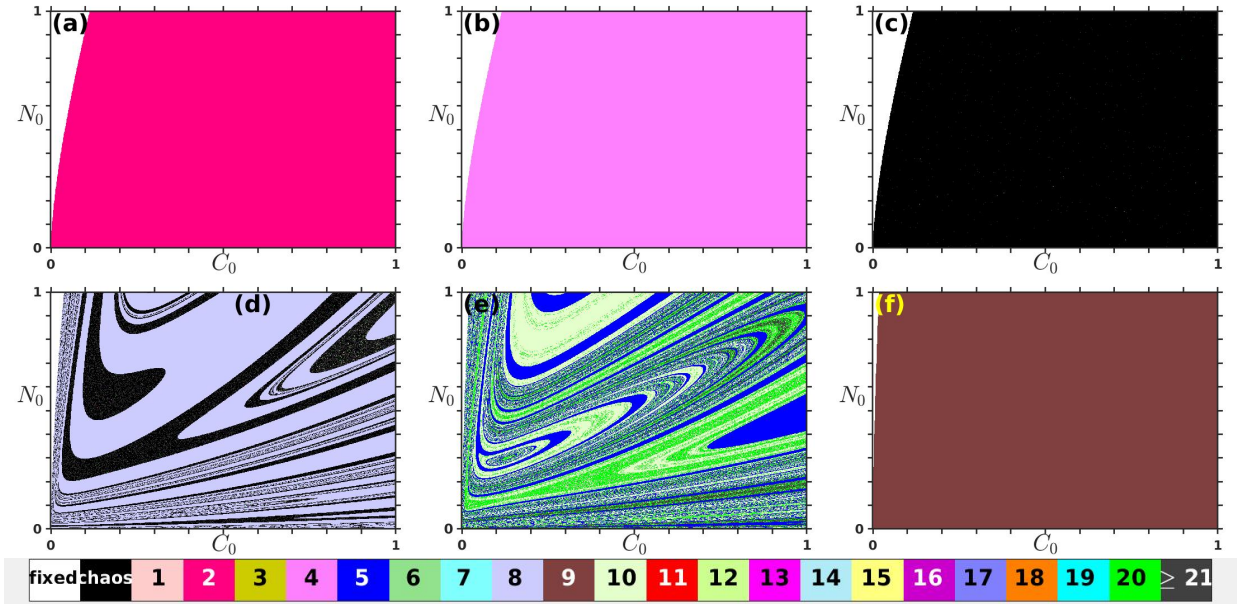
Figure 3: Basins of attraction N_0 vs. C_0 when no radiation is acting on the system and with $I(0) = 0.01$ obtained for different values of (a, d): (a) (1.383,3.177) (period-2), (b) (1.383,3.109) (period-4), (c) (1.383,3.096) (chaos), (d) (1.103,2.499) (period-8) for the planes in Fig. 2(a) and (b) respectively. (e) (1.054,2.308) (period-5 and its multiples). (f) (1.054,2.285) (period-9). Other parameters values are as in Fig. 2.

the initial conditions $(C(0), N(0), I(0)) = (0.9, 0.09, 0.01)$, we get a stable limit cycle with one isospike per period (period-1). The treatment begins after $t_0 = 400$ hours to ensure convergence to the limit cycle. We observe that after the irradiation, the system recovers its original dynamics as shown in Figs. 4(b), and (d)–(e). The attractors into the phase space for perturbed (considering the radiation action) and unperturbed situations are depicted in Fig. 4(c). Nevertheless, Figs. 4(d)–(e) transiently converges to an apparently stable fixed point in the intervals [880, 1222] and [640, 2132] hours respectively, but followed by an inversion in the presence of the predominant cells, and eventually, the system recovers its original dynamics. The attractors related to the perturbed and unperturbed time series of Fig. 4(e) are represented in Fig. 4(f). We have not found a situation with persistent fixed point stability when varying the treatment features. It is noticeable that the treatment seems to eliminate the cancerous cells in a transitory way; however, after a specific time, the original behavior is recovered. The transitory time in which the cancerous cells are removed depends on how the total dose is delivered; few sessions and consequently higher doses per session enlarge such time.

When working with a point in the parameter plane corresponding to a stable limit cycle with each period containing two isospikes ($a = 0.93$, $d = 1.8$) and the same treatment protocol as in Figs. 3(b) and (c), we observe similar features in the dynamical behavior than in the precedent case (see Fig. 5). There are only transitory times when the cancerous cells are almost eliminated, and such times strongly depend on the irradiation protocol. At this stage,
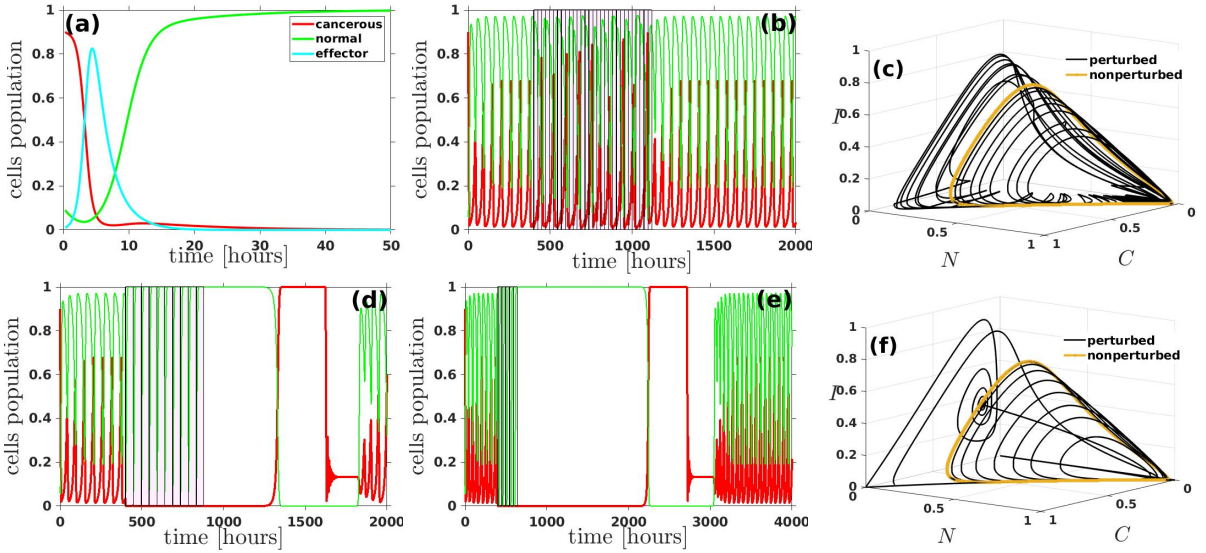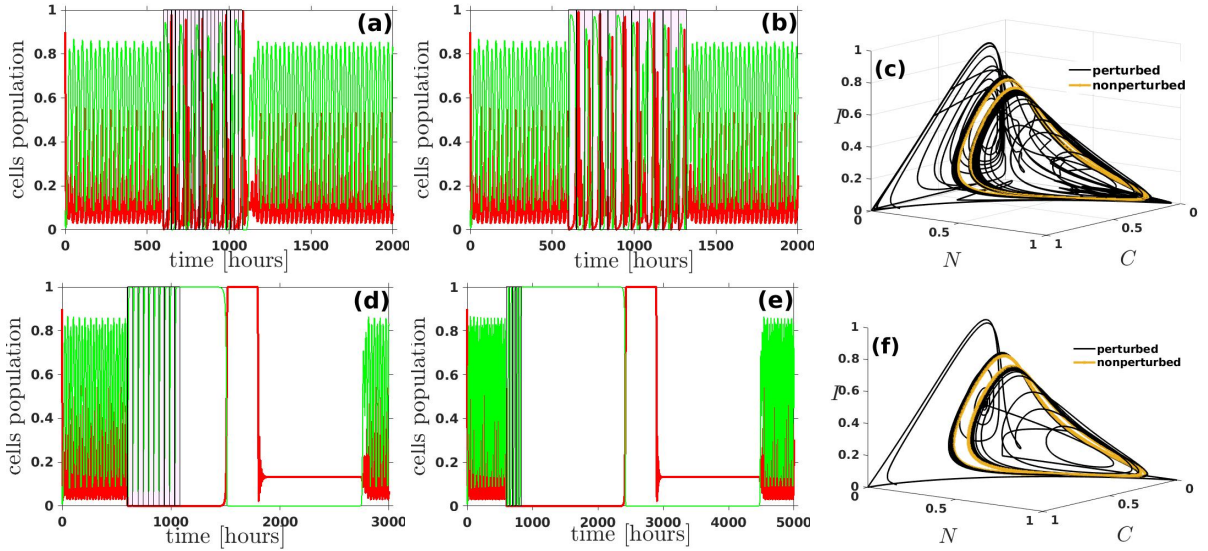
Figure 4: Fixed point and period-1 oscillations. (a), (b), (d), (e), time series with initial conditions $(C(0), N(0), I(0)) = (0.9, 0.09, 0.01)$ when (a) $a = d = 1.1$ corresponding to a fixed point stability, and (b), (d), (e) $a = d = 0.93$ (stable limit cycle with one isospike per period) when the following irradiation protocols are applied: (b) $t_0 = 400$ hr, $n = 30$, $\Delta T = 24$ hr, (d) $t_0 = 400$ hr, $n = 10$, $\Delta T = 48$ hr, and (e) $t_0 = 400$ hr, $n = 5$, $\Delta T = 48$ hr. The attractors in panels (c) and (f) correspond to the cases (b) and (e), respectively, with the perturbation effects (black) and the original nonperturbed limit cycle (orange). Note that in all cases, $D_T = 60$ Gy and $\dot{D} = 3$ Gy/min. The parameters related to the irradiation are $p = 0.3$, and r is computed with Eqs. (4)–(5). For clarity, in the time series plot (b), (d), and (e), we only represent C and N.

it is important to realize that at the end of the above-mentioned transitory time in which the cancerous cells have been almost eliminated, there is an abrupt transition consisting of the populations' inversion, i.e., the cancerous cells population surges radically, and the healthy cells population slumps dramatically. These facts are related to the oscillation and amplitude death phenomena [66].

Thus, as in Fig. 4(b) in Figs. 5(a)–(b), it is not possible to attain the stationary situation in which the normal cells survive, and the cancerous ones tend to disappear. In Figs. 5(d)– (e), we observe the same behavior as in Fig. 4(d)– (e), i.e., there is a transitory, apparently stable fixed point in which normal cells are predominant occurring in the time intervals [1062, 1365] hours (Fig. 4(d)) and [840, 2331] hours (Fig. 4(e)). Afterward, the original limit cycle is recovered.

As another example, we consider a point in the parameter plane corresponding to a period -3 oscillatory behavior with $(a, d) = (1.0, 1.9)$, the initial conditions $(C(0), N(0), I(0)) = (0.9, 0.09, 0.01)$, and the starting time of the treatment after 600 hours. In Fig. 6(a), we consider similar irradiation conditions as in the precedent cases ($n = 20$, $\Delta T = 24$ hr, and $D_T = 60$ Gy). Surprisingly, we found out that this irradiation protocol permanently eliminates cancerous cells, indicating that it might be adopted for efficient treatments. However, a slight change in the protocol, considering $\tau = 48$ hours, does not lead the system to remove cancerous cells. After the treatment, the system recovers
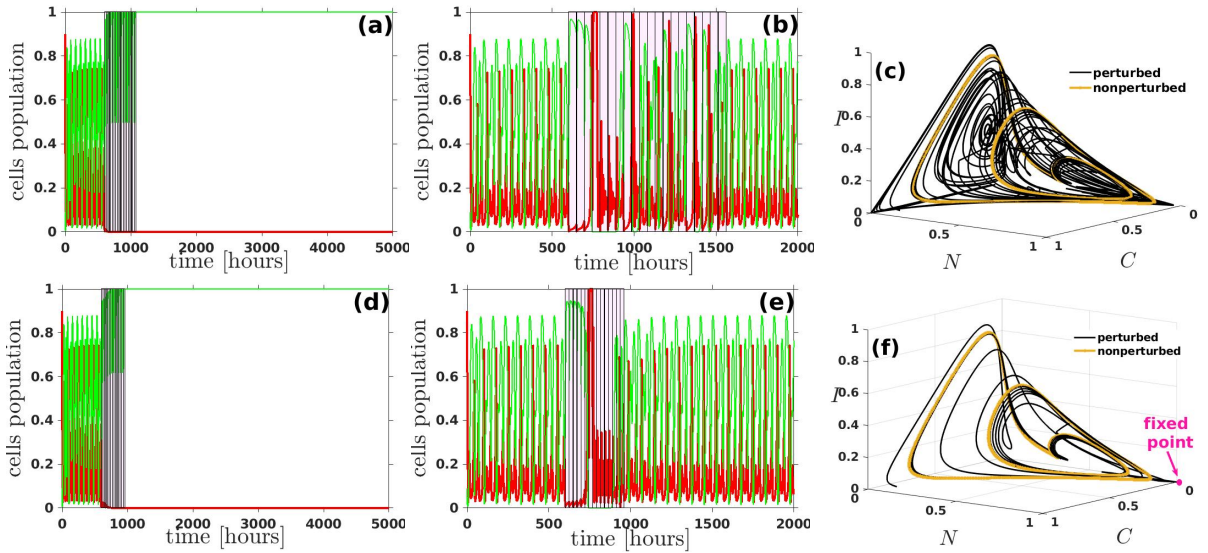
Figure 5: Period-2 oscillations. (a), (b), (d), (e), time series with initial conditions $(C(0), N(0), I(0)) = (0.9, 0.09, 0.01)$ when (a) $a = 0.93$ and $d = 1.8$ corresponding to a limit cycle stability, with two isospikes per period when the following irradiation protocols are applied: (a) $t_0 = 600$ hr, $n = 20$, $\Delta T = 24$ hr, (b) $t_0 = 600$ hr, $n = 15$, $\Delta T = 48$ hr, (d) $t_0 = 600$ hr, $n = 10$, $\Delta T = 48$ hr, and (e) $t_0 = 600$ hr, $n = 5$, $\Delta T = 48$ hr. The attractors in panels (c) and (f) correspond to the cases (b) and (e), respectively, with the perturbation effects (black) and the original nonperturbed limit cycle (orange). Note that in all cases, $D_T = 60$ Gy and $\dot{D} = 3$ Gy/min. The parameters related to the irradiation are $p = 0.3$, and r is computed with Eqs. (4)–(5). For clarity, in the time series panels, we only represent C and N.

its original period-3 behavior (see Fig. 6(b). The attractor corresponding to the whole time series of Fig. 6(b) (black) and the nonperturbed limit cycle (orange) are shown in Fig. 6(c). Based on the last results, we realize that it is possible to reduce significantly the total dose until $D_T = 37$ Gy and attain our goal of eliminating the cancerous cells with the protocol $n = 15$, $\Delta T = 24$ hr as it is shown in Fig. 6(d). Nevertheless, the same protocol but with $D_T = 36$ Gy does not lead to the removal of cancerous cells (see Fig. 6(e)). The attractor leading to a fixed point stability as that attained in Fig. 6(d) is represented in Fig. 6(f).

### 3.3. Radiation effects on chaotic dynamical behavior

As stated in Sect. 3.1, the system exhibits multistability, and for the same chosen parameters, it is possible to observe periodic/chaotic oscillations or a stable fixed point depending on the initial conditions. This multistability feature allows the possibility to lead the system towards certain dynamical behaviors and control it. Our goal is to attain fixed points where the cancerous cells are removed, and the aspects mentioned above permit a logical explanation of how to obtain the desired results. Let us start by considering the point in the parameter plane $(a, d) = (1.0, 1.327)$, and the initial conditions $(C(0), N(0), I(0)) = (0.9, 0.09, 0.01)$ corresponding to chaotic behavior. The starting time of the treatment might be chosen at any time since the chaotic behavior related to the transient and the intrinsic dynamic behavior are indistinguishable. Similarly to what is observed in Fig. 6(d), it is possible to change the standard protocol

Figure 6: Period-3 oscillations. (a), (b), (d), (e), time series with initial conditions $(C(0), N(0), I(0)) = (0.9, 0.09, 0.01)$ when $a = 1.0$ and $d = 1.9$ corresponding to a limit cycle stability with three isospikes per period) when the following irradiation protocols are applied: (a) $D_T = 60$ Gy, $n = 20$, $\Delta T = 24$ hr.(b) $D_T = 60$ Gy, $n = 20$, $\Delta_T = 48$ hr, (d) $D_T = 37$ Gy, $n = 15$, $\Delta T = 24$ hr, and (e) $D_T = 36$ Gy, $n = 15$, $\Delta T = 24$ hr. The attractors in panels (c) and (f) correspond to the cases (b) and (e), respectively, with the perturbation effects (black) leading to restore the stable limit cycle of period-3 (orange) and the case in which the radiation action leads to a stable fixed point with predominancy of healthy cells. In all cases, the dose rate is $\dot{D} = 3$ Gy/min. The parameters related to the irradiation are $p = 0.3$, and r is computed with Eqs. (4)–(5). For better insight, in the time series plots (a)–(d) and (d)–(e), we only represent C and N.

stipulating a total dose of 60 Gy to another one in which D_T is much less but permitting us to achieve the goal of eliminating cancerous cells. Thus, Fig. 7(a) corresponds to the time series with $D_T = 48$ Gy, $n = 30$, and $\Delta T = 24$ hr. When reducing the total dose to $D_T = 47$ Gy, the system recovers its chaotic behavior after the treatment, as shown in Fig. 7(b). The attractor corresponding to Fig. 7(a) and its tendency towards the fixed point is sketched in Fig. 7(c). With the change of the protocol and reducing the number of sessions to 20 and the total dose to $D_T = 31$ Gy, it is not possible to eliminate the cancerous cells (Fig. 7(d)). Increasing the total dose to $D_T = 32$ Gy (computed but not shown), the transitory time in which the normal cells survive and the cancerous cells almost disappear is comprised in the interval [477.5, 3679] hr. Subsequently, there is a populations' inversion that ends with the recovery of the chaotic oscillations in the system as it happens in Figs. 4(d)–(e). Thus, there is enough time to use adjuvant treatments in radiotherapy and avoid cell populations' inversion. Figure 7(e) exhibits the persistence of the result of eliminating cancerous cells at least until 10^4 hours (see Fig. 7(e)) when $D_T = 33$ Gy. Finally, in Fig. 7(f), the attractors related to nonperturbed and perturbed situations are shown Fig. 7(d).

The initial periodic behavior looks robust, and in general, after an oscillation death, the original periodic behavior is recovered. However, in some situations, a long-lasting predominance of normal cells is attained (cycle with three isospikes and chaos). In these cases, it is feasible to work with lower total doses to eliminate cancerous cells. In the
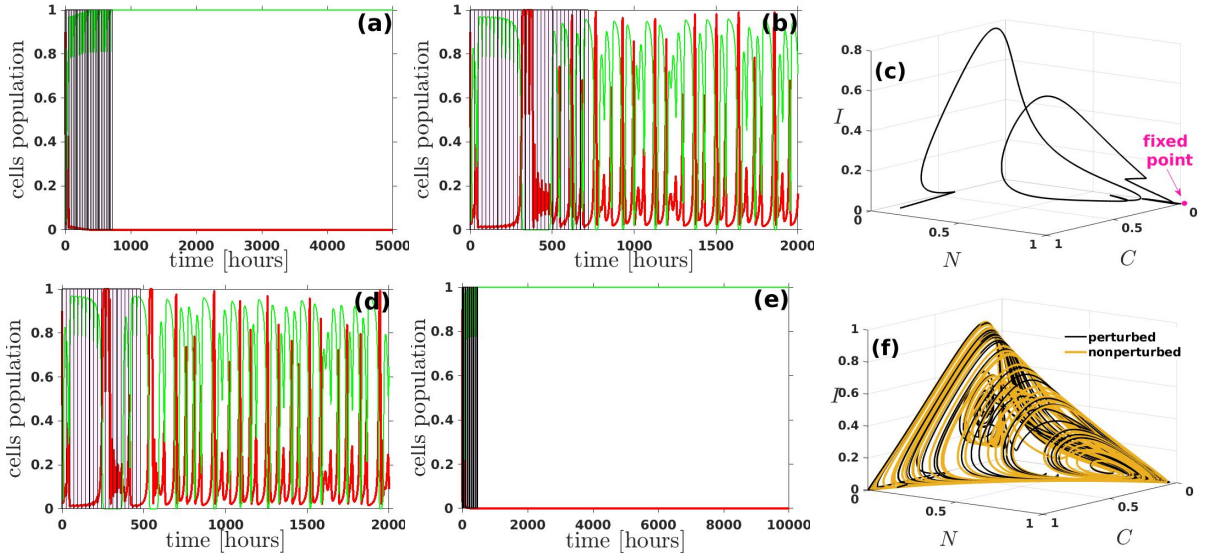
Figure 7: Chaotic oscillations. (a), (b), (d), (e), time series with initial conditions $(C(0), N(0), I(0)) = (0.9, 0.09, 0.01)$ when $a = 1.0$ and $d = 1.327$ corresponding to a chaotic attractor when the following irradiation protocols are applied: (a) $n = 30$, $\tau = 24$ hr, $D_T = 48$ Gy, (b) $n = 30$, $\tau = 24$ hr, $D_T = 47$ Gy, (d) $n = 20$, $\tau = 24$ hr, $D_T = 31$ Gy, and (e) $n = 20$, $\tau = 24$ hr, $D_T = 33$ Gy. The attractors in panels (c) and (f) correspond to the cases (a) and (d), respectively, with a stable fixed point in (c), and perturbed (black) and nonperturbed (orange) chaotic attractors in (f). As in Fig. 4, note that $\dot{D} = 3$ Gy/min. The parameters related to the irradiation are $p = 0.3$, and r is computed with Eq. (3). For better insight, in the time series plots (a)–(d) and (d)–(e), we only represent C and N.

case of initial chaotic behavior, eliminating cancerous cells is easier. The total dose, dose rate, number of sessions, and interval between two sessions play a significant role in obtaining different possible dynamics behavior. Eliminating cancerous cells is the main goal that might be achieved by modulating the abovementioned variables. Other interesting aspects from the dynamical systems viewpoint also arise, such as oscillation death, amplitude death, and resurrection of oscillations. The search for an optimal number of sessions for treatment is also possible. Our results suggest that not only radiological but chronobiological aspects in a treatment might play an important role. On the other hand, the outcomes are in accordance with new treatment tendencies [67, 68, 69], in which the treatment is personalized not only in the formulation of the protocol but also in what concerns the best timing of irradiation.

4. Conclusions and perspectives

We proposed a cell population model based on former models but introducing the periodically intermittent action of ionizing radiation as it happens in radiotherapy. We adapted the parameters to common values used in radiotherapy. The parameter plane analysis uncovered that a rich repertoire of dynamical behavior might be obtained when changing the values of the parameters quantifying the interaction of cancerous with healthy cells. The system indeed exhibits behaviors going from fixed points to chaos, including several regular regimes characterized by periodic oscillations with different numbers of isospikes.

The dynamical richness of the model is inspiring to contemplate some other aspects related to dynamical systems, such as the exploration of the parameter spaces as in [70], the basins of attraction, and the existence of amplitude and oscillation death followed by the resurrection of the oscillations.

We found an increased tendency to modify long-lastingly the dynamics of a system via the application of ionizing radiation when its initial dynamical behavior is chaotic. On the contrary, when the system initially exhibits periodic oscillatory behavior with one or two isospikes per period, it is more robust against the influence of ionizing radiation, recovering its original regularity after a specific time. These different responses to the ionizing radiation point to the importance of applying the radiation when the system is in a chaotic regime to eliminate cancerous cells.

The appropriate choice of the time in which the radiation is applied and the elapsed time between two irradiation sessions play an essential role in the effectiveness of the treatment. Consequently, reducing the total delivered dose and the number of treatment sessions is possible when the protocol considers the abovementioned aspects.

We are aware that a key aspect of a representative treatment is the careful determination of the control parameter values based on biological measurements. Nevertheless, these results reveal that the efficacy of an intermittent radiation treatment increases with the chaotic character of the cell population can be viewed as a general qualitative principle. Altogether, the results indicate that taking into account chronobiological aspects is important but not straightforward [71, 72]. The model might also be helpful for aspects related to radioprotection, especially concerning the biological effects of radiation on diverse types of cells.

The constancy of the parameters is a strong assumption; probably, during and after the irradiation, some parameters might vary due to biological mechanisms. From a mathematical viewpoint, time-varying parameters imply working with nonautonomous systems. This is out of our scope in this study, mainly because we need more information about such mechanisms.

As another limitation of this work, we only considered periodically intermittent radiation applications. As a perspective, we intend to tackle the problem when each session's delivered dose differs.

In summary, the apparently rather simple model used in this study exhibits a great dynamical richness. On the other hand, the combination of parameter planes and the modulation of the main variables of the treatment opens the possibility of improved treatments by reducing the number of sessions and the delivered total dose. Finally, the results further highlight that leading radiotherapy treatments toward a chronobiological approach is crucial.

Acknowledgements

References

[1] World Health Organization. WHO report on cancer: setting priorities, investing wisely andnproviding care for all. Geneva: World Health Organization; 2020. Available from: https://www.who.int/publications/i/item/9789240001299.

[2] Goldson AL. Cancer management in man: detection, diagnosis, surgery, radiology, chronobiology, endocrine therapy. vol. 9. Dordrecht: Springer; 1989. DOI: https://doi.org10.1007/978-94-009-2536-6.

[3] Withers HR. In: The Four R's of Radiotherapy. vol. 5 of Advances in Radiation Biology. New York: Academic Press; 1975. DOI: https://doi.org/10.1016/B978-0-12-035405-4.50012-8.

[4] Thames HD, Bentzen SM, Turesson I, Overgaard M, Van den Bogaert W. Time-dose factors in radiotherapy: a review of the human data. Radiother Oncol. 1990;19(3):219-35. DOI: http://dx.doi.org/10.1016/0167-8140(90)90149-Q.

[5] Moeller BJ, Richardson RA, Dewhirst MW. Hypoxia and radiotherapy: opportunities for improved outcomes in cancer treatment. Cancer Metast Rev. 2007;26(2):241-8. DOI: https://doi.org/10.1007/s10555-007-9056-0.

[6] Atun R, Jaffray DA, Barton MB, Bray F, Baumann M, Vikram B, et al. Expanding global access to radiotherapy. Lancet Oncol. 2015;16(10):1153-86. DOI: https://doi.org/10.1016/S1470-2045(15)00222-3.

[7] Major N, Patel NA, Bennett J, Novakovic E, Poloni D, Abraham M, et al. The Current State of Radiotherapy for Pediatric Brain Tumors: An Overview of Post-Radiotherapy Neurocognitive Decline and Outcomes. J Pers Med. 2022;12(7). DOI: https://doi.org/10.3390/jpm12071050.

[8] Rich TA, Shelton CH, Kirichenko A, Straume M. Chronomodulated chemotherapy and irradiation: an idea whose time has come? Chronobiol Int. 2002;19(1):191-205. DOI: https://doi.org/10.1081/CBI-120002598.

[9] Ershov YA, Kotin VV. Mathematical models of tumor processes and strategies of chemotherapy. In: Burlakova E, Shilov AE, Varfolomeev SD, Zaikov G, editors. Chemical and Biochemical Kinetics. New horizons vol. 1. Boca Raton: CRC Press; 2005. ch. 18. p. 302-21. ISBN: https://www.routledge.com/Chemical-kinetics/Burlakova-Shilov-Varfolomeev-Zaikov/p/book/9789067644303

[10] Kilgallen AB, Štibler U, Printezi MI, Putker M, Punt CJA, Sluijter JPG, May AM, van Laake LW. Comparing Conventional Chemotherapy to Chronomodulated Chemotherapy for Cancer Treatment: Protocol for a Systematic Review. JMIR Res Protoc. 2020;9(10):e18023. DOI: https://doi.org/10.2196/18023

[11] Walker WH, Sprowls SA, Bumgarner JR, Liu JA, Meléndez-Fernández OH, Walton JC, Lockman PR, DeVries AC, Nelson RJ. Circadian Influences on Chemotherapy Efficacy in a Mouse Model of Brain Metastases of Breast Cancer. Front Oncol. 2021;11:752331. DOI: https://doi.org/10.3389/fonc.2021.752331.

[12] Couzin-Frankel J. Cancer Immunotherapy. Science. 2013;342(6165):1432. DOI: https://doi.org/10.1126/science.342.6165.1432.

[13] Delitala M, Lorenzi T, Melensi M. Competition between cancer cells and T cells under immunotherapy: a structured population approach. ITM Web of Conferences. 2015;5:00005. DOI: https://doi.org/10.1051/itmconf/20150500005.

[14] Ghanizadeh M, Shariatpanahi SP, Goliaei B, Rüegg C. Mathematical modeling approach of cancer immunoediting reveals new insights in targeted-therapy and timing plan of cancer treatment. Chaos Soliton Fract. 2021;152:111349. DOI: https://doi.org/10.1016/j.chaos.2021.111349.

[15] Harrington K, Freeman DJ, Kelly B, Harper J, Soria JC. Optimizing oncolytic virotherapy in cancer treatment. Nat Rev Drug Discov. 2019;**18**(9):689-706. DOI: https://doi.org/10.1038/s41573-019-0029-0.

[16] Norton L. A Gompertzian model of human breast cancer growth. Cancer Res. 1988;48(24 Part 1):7067-71. Available from: https://aacrjournals.org/cancerres/article/48/24_Part_1/7067/493254/A-Gompertzian-Model-of-Human-Breast-Cancer-Growth1.

[17] Obcemea C. Chaotic Dynamics of Tumor Growth and Regeneration. In: Minai AA, Bar-Yam Y, editors. Unifying Themes in Complex Systems. Springer Berlin Heidelberg;. p. 349-54. DOI: https://doi.org/10.1007/978-3-540-35866-4_34.

[18] Castorina P, Deisboeck TS, Gabriele P, Guiot C. Growth Laws in Cancer: Implications for Radiotherapy. Radiat Res. 2007;**168**(3):349-56. DOI: https://doi.org/10.1667/RR0787.1.

[19] Rozenfeld HD, Rybski D, Andrade JS, Batty M, Stanley HE, Makse HA. Laws of population growth. P Natl Acad Sci USA. 2008;**105**(48):18702. DOI: https://doi.org/10.1073/pnas.0807435105.

[20] Bi P, Ruan S, Zhang X. Periodic and chaotic oscillations in a tumor and immune system interaction model with three delays. Chaos. 2014;**24**(2):023101. DOI: https://doi.org/10.1063/1.4870363.

[21] Xin Y, Cummins B, Gedeon T. Multistability in the epithelial-mesenchymal transition network. BMC Bioinformatics. 2020;**21**(1):71. DOI: https://doi.org/10.1186/s12859-020-3413-1.

[22] Singh PP, Roy BK. Chaos and multistability behaviors in 4D dissipative cancer growth/decay model with unstable line of equilibria. Chaos Soliton Fract. 2022;**161**:112312. DOI: https://doi.org/10.1016/j.chaos.2022.112312.

[23] Pisarchik AN, Hramov AE. Multistability in Physical and Living Systems. Cham: Springer; 2022. DOI: https://doi.org/10.1007/978-3-030-98396-3.

[24] Huang S, Ernberg I, Kauffman S. Cancer attractors: A systems view of tumors from a gene network dynamics and developmental perspective. Semin Cell Dev Biol. 2009;**20**(7):869-76. DOI: https://doi.org/10.1016/j.semcdb.2009.07.003.

[25] Li Q, Wennborg A, Aurell E, Dekel E, Zou JZ, Xu Y, Huang S, Emberg I. Dynamics inside the cancer cell attractor reveal cell heterogeneity, limits of stability, and escape. P Nat Acad Sci. 2016;**113**(10):2672-7. DOI: https://doi.org/10.1073/pnas.1519210113.

[26] Kuznetsov VA, Makalkin IA, Taylor MA, Perelson AS. Nonlinear dynamics of immunogenic tumors: Parameter estimation and global bifurcation analysis. B Math Biol. 1994;**56**(2):295-321. DOI:http://dx.doi.org/10.1007/BF02460644.

[27] Kirschner D, Panetta JC. Modeling immunotherapy of the tumor–immune interaction. J Math Biol. 1998;**37**(3):235-52. DOI: http://dx.doi.org/10.1007/s002850050127.

[28] Nani F, Freedman HI. A mathematical model of cancer treatment by immunotherapy. Math Biosci;**163**(2):159-99. DOI: http://dx.doi.org/10.1016/S0025-5564(99)00058-9.

[29] Freedman HI, Belostotski G. Perturbed models for cancer treatment by radiotherapy. Differ Equ Dyn Syst. 2009;**17**(1-2):115-33. DOI: http://dx.doi.org/10.1007/s12591-009-0009-7.

[30] Jiménez RP, Hernandez EO. Tumour-host dynamics under radiotherapy. Chaos Soliton Fract. 2011;**44**(9):685-92. DOI: https://doi.org/10.1016/j.chaos.2011.06.001.

[31] Liu Z, Yang C. A Mathematical Model of Cancer Treatment by Radiotherapy. Comput Math Method M. 2014;**2014**:172923. DOI: http://dx.doi.org/10.1155/2014/172923.

[32] Isea R, Lonngren KE. A Mathematical Model of Cancer Under Radiotherapy. Int J Public Health Res. 2015;**3**(6):340-4. Available from: http://www.openscienceonline.com/journal/archive2?journalId=718&paperId=2500.

[33] Ribba B, Colin T, Schnell S. A multiscale mathematical model of cancer, and its use in analyzing irradiation therapies. Theor Biol Med

Model. 2006;**3**(1):7. DOI: http://dx.doi.org/10.1186/1742-4682-3-7.

[34] Ghaffari A, Bahmaie B, Nazari M. A mixed radiotherapy and chemotherapy model for treatment of cancer with metastasis. Math Method Appl Sci. 2016;**39**(15):4603-17. DOI: https://doi.org/10.1002/mma.3887.

[35] Dingli D, Cascino MD, Josić K, Russell SJ, Bajzer Ž. Mathematical modeling of cancer radiovirotherapy. Math Biosci. 2006;**199**(1):55-78. DOI: https://doi.org/10.1016/j.mbs.2005.11.001.

[36] Roenneberg T, Klerman EB. Chronobiology. Somnologie. 2019;**23**:1-5. DOI: https://doi.org/10.1007/s11818-019-00217-9.

[37] Goldbeter A. Computational approaches to cellular rhythms. Nature. 2002;**420**(6912):238-45. DOI: https://doi.org/10.1038/nature01259.

[38] López AG, Seoane JM, Sanjuán MAF. A Validated Mathematical Model of Tumor Growth Including Tumor–Host Interaction, Cell-Mediated Immune Response and Chemotherapy. B Math Biol. 2014;**76**(11):2884-906. DOI: http://dx.doi.org/10.1007/s11538-014-0037-5.

[39] Altinok A, Lévi F, Goldbeter A. A cell cycle automaton model for probing circadian patterns of anticancer drug delivery. Adv Drug Deliver Rev. 2007;**59**(9):1036-53. DOI: https://doi.org/10.1016/j.addr.2006.09.022.

[40] Bernard S, Čajavec Bernard B, Lévi F, Herzel H. Tumor Growth Rate Determines the Timing of Optimal Chronomodulated Treatment Schedules. PLOS Comput Biol. 2010 03;**6**(3):1-11. DOI: https://doi.org/10.1371/journal.pcbi.1000712.

[41] Ballesta A, Dulong S, Abbara C, Cohen B, Okyar A, Clairambault J, Lévi F. A Combined Experimental and Mathematical Approach for Molecular-based Optimization of Irinotecan Circadian Delivery. PLOS Comput Biol. 2011;**7**(9):1-12. https://doi.org/10.1371/journal.pcbi.1002143.

[42] Hill RJW, Innominato PF, Lévi F, Ballesta A. Optimizing circadian drug infusion schedules towards personalized cancer chronotherapy. PLOS Comput Biol. 2020;**16**(1):e1007218 DOI: https://doi.org/10.1371/journal.pcbi.1007218.

[43] Hesse J, Martinelli J, Aboumanify O, Ballesta A, Relógio A. A mathematical model of the circadian clock and drug pharmacology to optimize irinotecan administration timing in colorectal cancer. Comput Struct Biotechnol J. 2021;**19**:5170-83. DOI: https://doi.org/10.1016/j.csbj.2021.08.051.

[44] Sachs RK, Hlatky LR, Hahnfeldt P. Simple ODE models of tumor growth and anti-angiogenic or radiation treatment. Math Comput Model. 2001;**33**(12):1297-305. DOI: https://doi.org/10.1016/S0895-7177(00)00316-2.

[45] Pinho STR, Freedman HI, Nani F. A chemotherapy model for the treatment of cancer with metastasis. Math Comput Model. 2002;**36**(7-8):773-803. DOI: http://dx.doi.org/10.1016/S0895-7177(02)00227-3.

[46] De Pillis LG, Radunskaya A. Modeling and Simulation of Tumor Development, Treatment, and Control. The dynamics of an optimally controlled tumor model: A case study. Math Comput Model. 2003;**37**(11):1221-44. DOI: http://dx.doi.org/10.1016/S0895-7177(03)00133-X.

[47] Belostotski G, Freedman H. A control theory model for cancer treatment by radiotherapy. Int J Pure Appl Math;**25**(4):447-80. Available from: http://www.ijpam.eu/contents/2005-25-4/3/index.html.

[48] de Pillis LG, Gu W, Radunskaya AE. Mixed immunotherapy and chemotherapy of tumors: modeling, applications and biological interpretations. J Theor Biol. 2006;**238**(4):841-62. DOI: http://dx.doi.org/10.1016/j.jtbi.2005.06.037.

[49] Itik M, Banks SP. Chaos in a Three-Dimensional Cancer Model. Int J Bifurcat Chaos. 2010;**20**(01):71-9. DOI: http://dx.doi.org/10.1142/S0218127410025417.

[50] Liu Z, Zhong S, Yin C, Chen W. Permanence, extinction and periodic solutions in a mathematical model of cell populations affected by

periodic radiation. Appl Math Lett. 2011;**24**(10):1745-50. DOI: http://dx.doi.org/10.1016/j.aml.2011.04.036.

[51] Saleem M, Agrawal T. Chaos in a Tumor Growth Model with Delayed Responses of the Immune System. J Appl Math. 2012;**2012**:891095. DOI: https://doi.org/10.1155/2012/891095.

[52] Letellier C, Denis F, Aguirre LA. What can be learned from a chaotic cancer model? J Theor Biol. 2013;**322**:7-16. DOI: http://dx.doi.org/10.1016/j.jtbi.2013.01.003.

[53] Borges FS, Iarosz KC, Ren HP, Batista AM, Baptista MS, Viana RL, Lopes SR, Grebogi C. Model for tumour growth with treatment by continuous and pulsed chemotherapy. Biosystems. 2014;**116**:43-8. DOI: https://doi.org/10.1016/j.biosystems.2013.12.001.

[54] Galindo MC, Nespoli C, Messias M. Hopf Bifurcation, Cascade of Period-Doubling, Chaos, and the Possibility of Cure in a 3D Cancer Model. Abstr Appl Anal. 2015;**2015**:11. DOI: http://dx.doi.org/10.1155/2015/354918.

[55] Dokuyucu MA, Celik E, Bulut H, Baskonus HM. Cancer treatment model with the Caputo-Fabrizio fractional derivative. Eur Phys J Plus. 2018;**133**(3):92. DOI: https://doi.org/10.1140/epjp/i2018-11950-y.

[56] Awadalla M, Yameni YY, Abuassba K. A new fractional model for the cancer treatment by radiotherapy using the Hadamard fractional derivative. Online Math. 2019;**1**:14-8. DOI: https://doi.org/10.5281/zenodo.3046037

[57] Das P, Upadhyay RK, Das P, Ghosh D. Exploring dynamical complexity in a time-delayed tumor-immune model. Chaos. 2020;**30**(12):123118. DOI: https://doi.org/10.1063/5.0025510.

[58] Farayola MF, Shafie S, Siam FM, Khan I. Mathematical modeling of radiotherapy cancer treatment using Caputo fractional derivative. Comput Meth Prog Bio. 2020;**188**:105306. DOI: https://doi.org/10.1016/j.cmpb.2019.105306.

[59] Ramírez-Ávila GM. Theoretical study of the action of ionizing radiations on the cancer cells population dynamics in Spanish]. Revista Boliviana de Física. 2017;**31**:25-34. Available from: http://www.scielo.org.bo/scielo.php?script=sci_abstract&pid=S1562-38232017000200004&lng=es&nrm=iss&tlng=es.

[60] Bashkirtseva I, Ryashko L, L'opez ÁG, Seoane JM, Sanju'an MAF. The effect of time ordering and concurrency in a mathematical model of chemoradiotherapy. Commun Nonlinear Sci. 2021;**96**:105693. DOI: https://doi.org/10.1016/j.cnsns.2021.105693.

[61] Rodrigues G, Choy H, Bradley J, Rosenzweig KE, Bogart J, Curran JW Jr, Gore E, Langer C, Louie AV, Lutz S, Machtay M, Puri V, Werner-Wasik, M, Videtic GMM. Definitive radiation therapy in locally advanced non-small cell lung cancer: Executive summary of an American Society for Radiation Oncology (ASTRO) evidence-based clinical practice guideline. Pract Radiat Oncol. 2015;**5**(1879-8519 (Electronic)):141-8. DOI: http://dx.doi.org/10.1016/j.prro.2015.02.012.

[62] Grassberger C, Paganetti H. Methodologies in the modeling of combined chemo-radiation treatments. Phys Med Biol;**61**(21):R344-67. DOI: http://dx.doi.org/10.1088/0031-9155/61/21/R344.

[63] Huo M, Rose M, van Prooijen M, Cusimano MD, Laperriere N, Heaton R, Gentili F, Payne D, Shultz DB, Kongkham P, Kalia SK, Schwartz M, Bernstein M, Spears J, Zadeh G, Hodaie M, Tsang DS. Importance of Cobalt-60 Dose Rate and Biologically Effective Dose on Local Control for Intracranial Meningiomas Treated With Stereotactic Radiosurgery. Neurosurgery;**90**(1524-4040 (Electronic)):140-7. DOI: https://doi.org/10.1227/neu.0000000000001755.

[64] Gallas MR, Gallas MR, Gallas JAC. Distribution of chaos and periodic spikes in a three-cell population model of cancer. Eur Phys J-Spec Top. 2014;**223**(11):2131-44. DOI: http://dx.doi.org/10.1140/epjst/e2014-02254-3.

[65] Pisarchik AN, Feudel U. Control of multistability. Phys Rep. 2014;**540**(4):167-218. DOI: http://dx.doi.org/10.1016/j.physrep.2014.02.007.

[66] Koseska A, Volkov E, Kurths J. Oscillation quenching mechanisms: Amplitude vs. oscillation death. Phys Rep. 2013;**531**(4):173-99. DOI:

http://dx.doi.org/10.1016/j.physrep.2013.06.001.

[67] Harper E, Talbot CJ. Is it Time to Change Radiotherapy: The Dawning of Chronoradiotherapy? Clin Oncol. 2019;**31**(5):326-35. DOI: https://doi.org/10.1016/j.clon.2019.02.010.

[68] Shuboni-Mulligan DD, Breton G, Smart D, Gilbert M, Armstrong TS. Radiation chronotherapy—clinical impact of treatment time-of-day: a systematic review. J Neuro-Oncol. 2019;**145**(3):415-27. DOI: https://doi.org/10.1007/s11060-019-03332-7.

[69] Hassan SA, Ali AAH, Sohn D, Flögel U, Jänicke RU, Korf HW, von Gall C. Does timing matter in radiotherapy of hepatocellular carcinoma? An experimental study in mice. Cancer Med-US. 2021;**10**(21):7712-25. DOI: https://doi.org/10.1002/cam4.4277.

[70] Ramírez-Ávila GM, Kurths J, Gallas JAC. Ubiquity of ring structures in the control space of complex oscillators. Chaos. 2021;**31**(10):101102. DOI: https://doi.org/10.1063/5.0066877.

[71] Halberg F, Halberg J, Halberg E, Halberg F. In: Goldson AL, editor. Chronobiology, Radiobiology and Steps Toward the Timing of Cancer Radiotherapy. Dordrecht: Springer Netherlands; 1989. p 227-53. DOI: https://doi.org/10.1007/978-94-009-2536-6_19.

[72] Haus E. Chronobiology of the mammalian response to ionizing radiation potential applications in oncology. Chronobiol Int. 2002;**19**(1):77-100. DOI: https://doi.org/10.1081/CBI-120002592.